

COVER PAGE

Document downloaded by @DAEL

Sat Nov 28 22:34:20 2026
For personal use

When automatic English translation is provided, only the original document is authentic.
The EAA cannot be held responsible of any translation error

Bibliographical reference

Locally Reacting Impedance in a Digital Waveguide Mesh by Mixed Modeling Strategies for Room Acoustic Simulation, José Escolano, José J. López and Basilio Pueo, Acta Acustica **vol. 95** (Number 6), 2009, pp. 1048-1059

DOI
https://doi.org/10.3813/AAA.918237

ACTA ACUSTICA UNITED WITH ACUSTICA
Vol. 95 (2009) 1048 – 1059

DOI 10.3813/AAA.918237

Locally Reacting Impedance in a Digital Waveguide Mesh by Mixed Modeling Strategies for Room Acoustic Simulation

José Escolano[1,2], José J. López[2], Basilio Pueo[3]

[1] Telecommunication Engineering Department, University of Jaén, 23700, Linares, Spain

[2] Institute for Telecommunication and Multimedia Applications, Universidad Politécnica de Valencia, 46021 Valencia, Spain

[3] Polytechnic School, University of Alicante, 03690 Alicante, Spain.

escolano@ujaen.es; jjlopez@dcom.upv.es; basilio@ua.es

Summary

The Digital Waveguide Mesh is a numerical approach for modelling sound field propagation in acoustic systems. One of the most important reasons for using this method lies in the possibility to include boundary conditions in a simple way. However, these methods do not fit into any standard impedance model, which reduces the accuracy of the whole method. In this paper, a new approach is proposed in order to accurately simulate impedance behavior, particularly a locally reacting impedance. The proposed model places special emphasis on the frequency dependent impedance case. This impedance definition is commonly used to characterise plane surfaces. The results demonstrate how accurate the proposed realisation is, compared to theory and how the simulations obtained outperform previously proposed methods.

PACS no. 43.20.Px, 43.20Fn, 43.55.Ka

1. Introduction

The Digital Waveguide Mesh (DWM) is a numerical model for acoustic simulation, with a promising use in room acoustics [1]. This method computes a discretised version of the D'Alembert solution of the wave equation by taking into account the specific initial and boundary conditions of the particular medium. It provides fast and accurate solutions and its relevance has grown with the power of computers. The DWM should be considered because it offers some advantages when compared with other time-domain methods [2, 3]. These advantages are related to the possibility to plug in digital filters directly into the method. This then allows engineers to consider, for example, air absorption, frequency-dependent boundary conditions, diffuse surfaces, etc [1].

The main reason for choosing the DWM method instead of other wave-based methods, such as the finite difference time domain (FDTD) method [4], is based on its inherent ability to adapt both frequency dependent or independent boundary conditions [5, 6]. DWM relies on the characterisation of the reflection factor by means of a digital filter, which works properly for the 1-D problem [7]. However, it has been demonstrated that in the multidimensional case, this solution does not correspond to any impedance model [8].

Although several solutions to diffuse surfaces have been successfully proposed [9], specular reflections are not accurately modelled in a multidimensional DWM. For that reason, it is necessary to propose a method which include, in a simple and efficient way, realistic models of impedance on the simulation such as the locally reacting impedance, despite being no explicit information about the particle velocity components. This model would improve the accuracy of the whole acoustic simulation system. The locally reacting impedance is particularly important because it facilitates the modelling of specular reflections, due to the fact that the impedance value is not dependent on the wave angle of arrival and it has a considerable advantage over models that take explicit account of the mechanical properties of the surface [10].

In this paper, a realisation based on the interaction of a DWM with an impedance in terms of Wave Digital Filters [11] is proposed, in order to overcome the limitation of using reflection factor filters [5]. Although the use of mixed paradigms is not new [12], it will be analytically demonstrated that with the proper adaptation between both models, the results become a locally reacting impedance. This model provides more accurate results and therefore improves the global room acoustic simulation.

This paper is organized as follows: section 2 presents a brief overview of the DWM. section 3 provides a mathe-

Received 1 August 2008,
accepted 31 July 2009.

© S. Hirzel Verlag · EAA

matical review of the locally reacting impedance and discusses the problem of the DWM regarding the assumption of the local reaction. In section IV, the boundary condition realisation is introduced, this includes a detailed analysis that demonstrates its locally reacting impedance behavior. Finally, some examples will illustrate the accuracy of the presented method.

2. The digital waveguide mesh

The theory of the DWM is based on decomposing the solution to the wave equation into travelling (or diverging and converging) waves, in a similar fashion to the D'Alembert solution of the wave equation [10]. In an ideal lossless medium, the wave equation can be implemented by means of pure delays, and the total sound field is obtained by adding these travelling wave components.

The basis of the DWM arises from the Digital Wave Guide (DWG) method proposed to solve the 1-D wave equation [13]. This can be seen as a decomposition into a direct wave, and a reflected wave, in a medium with the speed of sound c. Each travelling wave can be simulated by a shift register using pure or fractional delays [14]. In this way, the digital waveguide is obtained by sampling both space and time. Spatial sampling points are known as *scattering junctions* in technical literature.

In the multidimensional case, the possible wave directions are an infinite number. In order to simplify the method, the first approach is to consider only the characteristic directions, derived from the cartesian DWM [2]. In Figure 1, the scattering junction $p_J(n)$ of a generic DWM, at a discrete time step n, is illustrated based on digital signal processing theory where scattering junctions are joined using digital delays. This junction is linked by means of bidirectional unit-delays to N neighbouring scattering junctions defined with index κ, where $\kappa = 1, \ldots, N$ (see Figure 1). The discrete pressure value $p_J(n)$, is located at the center of the figure, and is surrounded by N neighbouring scattering junctions, which are represented by $p_\kappa(n)$ ($\kappa = 1, \ldots, N$).

Let the signal $p^+_{J,\kappa}(n)$ be an incoming signal from the neighbouring junction κ and $p^-_{J,\kappa}(n)$ be an outgoing component. Note that delay lines $p^+_{J,\kappa}(n)$ and $p^-_{J,\kappa}(n)$ join $p_J(n)$ and $p_\kappa(n)$ (see Figure 1).

In a lossless medium and where only plane waves are considered, the Kirchhoff laws must hold

1. The sum of incoming particle velocities is equal to the sum of outgoing particle velocities at each junction.
2. The pressures in all crossing waveguides are equal at the junction.

According to these laws, the sound pressure at a given scattering junction is obtained [2, 1].

This model is also known as *Wave*-DWM or W-DWM, which arises as a contraposition to the *Kirchhoff*-DWM (or K-DWM) [7, 15, 16]. K-DWM can be obtained directly from the finite difference time domain (FDTD) approach of the wave equation [4, 17] or by means of the appropriate transformation of the W-DWM [18]. This approach is only dependent on the pressure in the scattering junction, not on the incoming and outgoing components. Both approaches are equivalent [15]; however, in terms of efficiency, K-DWM reduces the computational cost considerably, whereas the W-DWM has traditionally been used to adapt boundary conditions to the DWM [5]. In this paper, the nomenclature DWM makes reference to the W-DWM.

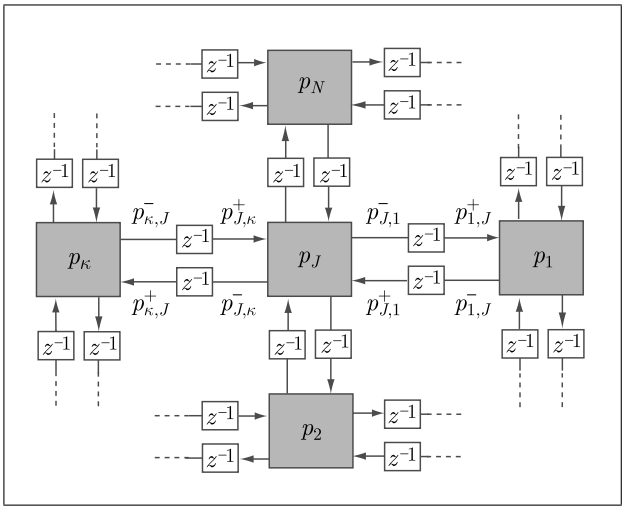

Figure 1. A digital waveguide mesh implementation of a 2-D Cartesian mesh through digital signal processing theory.

Let Δx and Δy be the spacing distances between the scattering junctions or spatial sampling, and Δt be the sampling period. These values must fulfill a relation in order to maintain the stability of the algorithm. In the DWM case, both K- and W-DWM, the relation between these quantities is the same as with the FDTD method. This stability condition is known as the Courant condition [4],

$$\Delta t \leq \frac{1}{c\sqrt{(1/\Delta x)^2 + (1/\Delta y)^2}}. \tag{1}$$

3. The locally reacting impedance problem

In this section, the locally reacting impedance problem is presented. The first subsection reviews the physical fundamentals related to these particular kinds of impedances. The second subsection revisits the problem of defining locally reacting impedances in a DWM.

3.1. Locally reacting surfaces

The normal surface specific acoustic impedance, or the specific boundary impedance for short, is defined for a given plane wave, as the ratio of complex amplitude and the normal component of the associated particle velocity. Let us consider a plane surface with a specific boundary impedance. This impedance presents a particular response depending on the shape of the incident wave. This is because the normal component of the particle velocity at any

point of the surface is influenced not only by the local pressure, but also by the surrounding points, meaning that it is not possible to specify a unique boundary impedance, independent of the amplitude and phase distribution of the incident wave over the surface [19].

However, there are cases where material is able to dissipate energy efficiently, i.e. porous sound absorbing materials [20], or where only reflection phenomena exists, i.e. ground surfaces [21]. In these scenarios it is reasonable to assume that the particle velocity generated by incident sound at any point is linearly related only to the *local* sound pressure, and then, independent of the shape of the incident sound field. Therefore, a material surface may be characterised in terms of a unique specific boundary impedance. Fortunately, this impedance can be considered in many practical cases, i.e. room acoustics [22].

Let us consider an infinitely extended impedance surface of uniform impedance. On the basis of a locally reacting impedance, it is possible to obtain a general expression for the reflection factor in terms of the impedance and the angle of the harmonic plane wave incidence. Let us define an incident plane wave with amplitude $\tilde{p}_{\text{inc}}$ and angular frequency ω, propagating in a direction $(\cos\theta, \sin\theta)$ where θ is the angle with the x-axis and approaching from $x < 0$ and impedance wall $Z = \tilde{p}/\tilde{u}_x$ at $x = 0$. On the other hand, The reflected wave, with amplitude $\tilde{p}_{\text{ref}}$, is propagating in the direction $(-\cos\theta, \sin\theta)$.

Both amplitudes are related to the reflection factor R

$$R = \tilde{p}_{\text{ref}}/\tilde{p}_{\text{inc}}. \tag{2}$$

Thus, the total pressure field p is the sum of both components (incident and reflected) and using the linearized momentum conservation law $\rho(\partial u_x/\partial t) = -\partial p/\partial x$, the normal component of the particle velocity u_x can be derived.

Once, both pressure and the normal component of the particle velocity is obtained, it permits the definition of the plane wave impedance at the point $x = 0$ and the reflection factor [22],

$$Z = \frac{\rho c}{\cos\theta}\frac{1+R}{1-R} \quad \text{or} \quad R = \frac{Z\cos\theta - \rho c}{Z\cos\theta + \rho c}, \tag{3}$$

An impedance with a local reaction assumption or locally reacting impedance, means that the impedance does not depend on the plane wave angle arrival, e. g. $Z = Z(\omega)$, but the reflection factor does depend on this angle, e. g. $R = R(\theta, \omega)$.

From equation (3), it can be observed that when the impedance has low values (high absorption), there are significant differences when the angle of arrival varies. However, if the impedance value increases (low absorption), the dependence on the angle of arrival decreases, especially for low angles of arrival where the reflection factor is almost constant at 0 dB. In this case, the highest differences appear when the angle tends to be parallel to the surface. When impedance tends to infinity, the reflection factor will be 0 dB for all the angles of incidence.

3.2. The locally reacting impedance problem in a DWM

One of the advantages of the DWM is the ease with which frequency-dependent boundary conditions can be included in the simulation. This is done by connecting a boundary filter that represents the reflection coefficient in each node [5]. The filter can be determined by digital transformation of the corresponding analytical expression [23]. This makes it possible to have different impedance conditions at each point on the boundaries.

However, as shown in section 3.1 a locally reacting surface with a specific impedance of $Z(\omega)$ has a plane wave reflection factor $R(\theta, \omega)$ which depends on the angle of incidence.

Since the angle of incidence θ is generally unknown, normal incidence is usually assumed [5]. In other words, with a given analytical impedance or with an impedance determined experimentally, the reflection factor filter is obtained by assuming null θ. If a plane wave arrives at the boundary with an angle of incidence θ, the filter simply has no knowledge of this angle. According to this, and even observing some dependence of the reflection factor with the angle of arrival, the impedance obtained does not correspond with a locally reacting model [8]. Therefore, in order to obtain a locally reacting impedance, the key point of this work is to directly couple the DWM with a discrete representation of a fixed impedance, rather than with the reflection factor; as a consequence, a locally reacting impedance will be achieved.

In accordance with the assumption of a locally reacting impedance where only plane waves must be considered, some considerations should be made about this point. Let us consider an incident plane wave according the assumptions of section 3.1, at a particular instant $n = t/\Delta t$. Now, consider the pressure in a scattering junction $p_J(n)$ located very close to the interface with the impedance surface and where the plane wave has struck [22]. According to this and the second Kirchhoff law (section 2)

$$\begin{aligned} p_J(n) &= \tilde{p}_{\text{inc}}(n) + \tilde{p}_{\text{ref}}(n) \\ &= p^+_{J,\kappa}(n) + p^-_{J,\kappa}(n) \quad \forall\kappa \in [1, \mathbb{N}]. \end{aligned} \tag{4}$$

One has to consider that equation (4) does not imply that $\tilde{p}_{\text{inc}}(n) = p^-_{J,\kappa}(n)$ or $\tilde{p}_{\text{ref}}(n) = p^+_{J,\kappa}(n)$. One should realise where in case $\tilde{p}_{\text{inc}}(n) = p^-_{J,\kappa}(n)$ could be considered, this would mean all outgoing κ components would be propagated with the same value and all incoming components would be constant and they would not depend on the neighboring junctions. Another example is when an incident plane wave travels; in that case, the term $\tilde{p}_{\text{ref}}(n)$ will be removed from equation (4); in that case, there exists incoming component, and thereby incoming and outgoing DWM components cannot be strictly identified with incident and reflected wave components. Of course, it should be emphasized how this equivalence would become true in the multidimensional case.

Although particle velocity components in the DWM are not explicitly calculated, they can be related directly to the

plane wave particle velocity by using a simple vector projection over the DWM axes. For instance, the total particle velocity over x-component (see Figure 1) is determined by

$$u_x(n) = \frac{\tilde{p}_{\mathrm{inc}}(n) - \tilde{p}_{\mathrm{ref}}(n)}{\rho c}\cos\theta = \frac{p^-_{J,1}(n) - p^+_{J,1}(n)}{Z_1}. \quad (5)$$

otherwise, the numerical particle velocity components would not fit with the definition of the real components. In equation (5), Z_1 is defined as the corresponding characteristic impedance between scattering junctions p_J and p_1.

It must be taken into account that the equality in equation (5) could not be completely accurate, due to the dispersion error, which depends on the frequency and angle [24]. However, if high enough oversampling is employed, the error can be assumed negligible. With this technique, equation (5) can be considered valid up to a fixed frequency. In practice, 2× oversampling is commonly used [2].

4. The Proposed Realization

As stated in the previous section, there is not a simple and efficient way to include the impedance in a DWM scheme in a global way. Therefore a combination of different methods may be the solution. Thus, the proposed method is based on the interaction between different paradigms: the impedance is modelled with a Wave Digital Filter (WDF) [11] and with the proper interaction model, it is coupled to the sound field space, a Digital Waveguide Mesh. This idea has been also explored in a staggered-FDTD scheme [25], where a WDF structure was used to represent a discrete-time impedance. However, it has to be taken into account that a DWM has no explicit information about the particle velocity components and this increases the difficulty to include locally reacting impedance, whereas a staggered FDTD scheme computes directly these particle velocity components. In this section, a review of the employed mixed modelling strategy is presented. In the next subsection, the proper model of the impedance is introduced and finally, the whole system is analyzed, demonstrating how the proposed realisation is able to simulate a locally reacting impedance.

4.1. Mixed modelling strategy

The mixed modelling strategy is a recent trend in digital sound synthesis by physical modelling, using different paradigms to simulate various parts of musical instruments [26, 27, 28]. Although in room acoustics this tendency is not usual, some works [7] and [29] have demonstrated that an efficient realisation of the DWM in room acoustics may be achieved just by mixing both K- (at the mesh itself) and W-DWM (at the boundaries) using KW-converters to mix both methods.

Based on this theory, this work addresses the coupling of a DWM method with a digital filter representing the impedance, rather than the reflection factor. The mixed modelling strategy for this coupling is the one proposed by Petrausch and Rabenstein [30]-[31]. They propose the use of WDF ports as a common interface between different blocks.

WDFs appear as a discretization process of complex systems, where each network element is discretized separately by a bilinear transformation [23]. The main reason for using WDFs as a common interface is the capacity to avoid potential computational problems, e.g., delay-free loops or potentially unstable implicit equations in the interconnection of the network elements [32]. This can be done by using of the so-called *wave variables*,

$$a_n(n) = p(n) + Z_p u_n(n), \quad (6)$$

$$b_n(n) = p(n) - Z_p u_n(n), \quad (7)$$

where the variables $a(n)$ and $b(n)$ represent the outgoing and incoming wave variables, respectively, and propagation information is inherent in them. The subindex n indicates that wave variables have the same direction as the component of the particle velocity u_n. In the same way, the Kirchhoff variables, p and u_n can be expressed in terms of the wave variables as

$$p(n) = \frac{a_n(n) + b_n(n)}{2}, \quad (8)$$

$$u_n(n) = \frac{a_n(n) - b_n(n)}{2Z_p}. \quad (9)$$

Originally, Fettweis defined these variables as voltage-current [11], but considering the *impedance analogy* [33] they can be used as acoustic variables. Moreover, the proper choice of the port resistance Z_p makes it possible to separate the design of the block elements from the definition of their interaction by appropriate adaptor elements [34]. Here, the nomenclature Z_p is used instead of the classic R for the resistance in order not to create confusion with the reflection factor. The separation and interaction in WDF terms ensures an unconditionally stable model provided when both parts, the DWM method of the sound field and the digital filter realisation of the impedance, are independently stable. Once delay-free loops are removed, the discrete-time domain system can be computed iteratively [11].

4.2. Impedance model

As stated above, the coupling between digital filters representing the impedance with WDF ports in this study has been realized using a certain model [30]. This solution is based on a Space State Systems (SSS) approach, which states that any linear system can be expressed in terms of an SSS.

In the present case a single input, $u_x(n)$, and a single output $p(n)$ are related as follows,

$$\mathbf{z}(n+1) = \mathbf{A}\mathbf{z}(n) + \mathbf{B}u_n(n), \quad (10)$$

$$p(n) = \mathbf{C}\mathbf{z}(n) + Du_n(n). \quad (11)$$

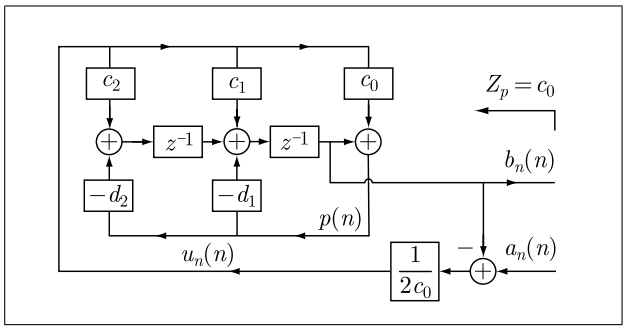

Figure 2. Interaction of a second order IIR filter with wave digital filter ports.

The vector $\mathbf{z}(n)$ is the system state. For this situation, $\mathbf{A}$ is a matrix, $\mathbf{B}$ and $\mathbf{C}$ are vectors, and D is a scalar (see reference [23] for more details).

Delay-free loops in the interconnection of the SSS with WDF are avoided by the following procedure: equation (11) is inserted into equations (6) and (7), and then is forced to $Z_p = D$ (see [30] for details). Then, $b(n)$ becomes independent of $u_n(n)$, avoiding instantaneous feedback and sources of instability. Thus,

$$u_n(n) = \frac{1}{2D}\big(a_n(n) - \mathbf{C}\mathbf{z}(n)\big), \tag{12}$$

$$b_n(n) = \mathbf{C}\mathbf{z}(n). \tag{13}$$

As an example, a second order IIR filter in a canonical observable form that represents the impedance is adapted to WDF ports. According to space state theory, a second order IIR digital filter is represented as an SSS by the equations

$$\mathbf{z}(n+1) = \begin{pmatrix} -d_1 & 1 \\ -d_2 & 0 \end{pmatrix} \mathbf{z}(n) + \begin{pmatrix} c_1 - c_0 d_1 \\ c_2 - c_1 d_2 \end{pmatrix} u_n(n)$$

$$p(n) = \begin{pmatrix} 1 & 0 \end{pmatrix} \mathbf{z}(n) + c_0 \cdot u_n(n). \tag{14}$$

The digital filter that represents the impedance expressed in terms of WDF ports is shown in Figure 2. Note that the specific impedance of the medium is always the independent term of the filter numerator polynomial, c_0.

4.3. Model description

In this section, the complete system is presented, explaining in detail the parts forming the whole system. Then, an analysis of the complete system will demonstrate its locally reacting impedance behaviour.

The most convenient and straightforward way to consider a frequency-dependent boundary condition is through a 1-D connection [5]. However, so far, the boundary condition has been expressed in terms of a reflection factor [8], where a constant angle of incidence is always assumed (see Figure 3a); the presented method proposes expressing it in terms of the impedance function itself (see Figure 3b), which is constant with any angle of incidence. Below, a frequency dependent impedance is assumed, giving a generalization of the boundary problem. It is important to note that although both schemes may look very similar, the scheme based on reference [5] uses a discrete-form

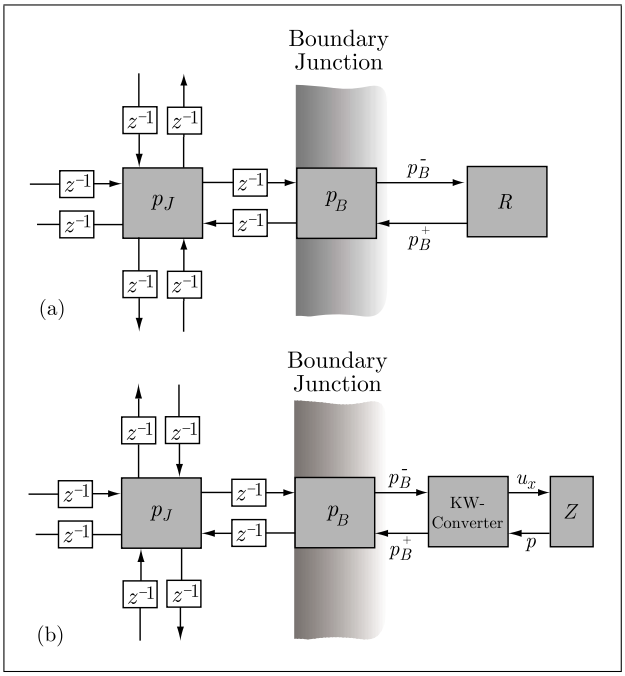

Figure 3. a: Termination of a waveguide mesh due to the boundary resulting in a reflection, where the boundary condition is expressed in terms of the reflectance R. b: Scheme of the proposed model, where the boundary condition is expressed in terms of the impedance Z.

of the reflection factor (which is not constant for the angle of incidence), whereas the impedance filter is constant for that angle of incidence, which is consequent with the definition of a locally reacting impedance (see section 3.1).

However, this interaction between the DWM and the impedance Z cannot consist of a direct connection for two main reasons: the first is related to the difference in the nature of the variables of each part; whereas the DWM is based on *wave* variables (there is a causal relationship between the incoming and outgoing wave components), the impedance is in terms of *Kirchhoff* variables (the impedance is defined as a ratio of two physical and observable variables). The second reason is the one mentioned in section 4.1, where the main source of instability in the coupling of two digital system is the delay-free loops. Fortunately, both handicaps are solved using a common interaction in terms of WDF.

It has to be noted how in the proposed method, the DWM sees the boundary condition as reflection factor as well, since the entrance to the boundary are wave variables. However, the main difference lies in the boundary condition definition, where the proposed method implicitly takes into account the angle of arrival, whereas the method of the Figure 3a assumes a certain unique angle, giving a non physical model.

At this point, the complete model is introduced in Figure 4. Once the conversion of the impedance filter in WDF ports has been solved in section 4.2, the DWM variables have to be converted as well. In the part of Figure 4, labelled as *DWM-WDF converter*, this process is carried out.

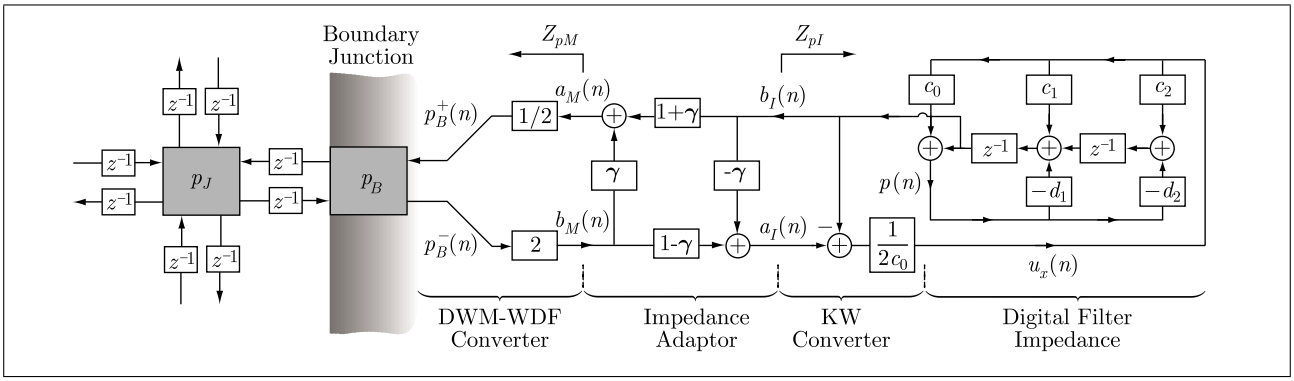

Figure 4. The completed proposed system. The DWM is connected with a digital filter realisation of the impedance through a variables adaptation, in order to avoid instabilities.

This is done by just identifying the DWM variables with WDF variables through a simple scaling factor [7, 35]:

$$p^+(n) = \frac{a(n)}{2}, \tag{15}$$

$$p^-(n) = \frac{b(n)}{2}. \tag{16}$$

Once both parts of the system are converted to WDF variables, it must be taken into account that each part has a different port resistance. This means that both parts cannot be directly connected. In order to couple these two WDFs and avoid instabilities, it is necessary to use a two-port adaptor (labelled as *impedance adaptor* in Figure 4) to adapt both WDF impedances and avoid direct feedback loops. This adaptor, known as *parallel adaptor* in WDF literature [36], relates wave variables to different impedance ports. A matrix description for a parallel adaptor of two WDF ports, M (subindex for the mesh) and I (subindex for the impedance), is

$$\begin{pmatrix} a_M(n) \\ a_I(n) \end{pmatrix} = \begin{pmatrix} \gamma & 1-\gamma \\ 1+\gamma & -\gamma \end{pmatrix} \begin{pmatrix} b_M(n) \\ b_I(n) \end{pmatrix}, \tag{17}$$

where $\gamma = (Z_{pM} - Z_{pI})/(Z_{pM} + Z_{pI})$.

In the particular case of the specific impedance of the mesh, Z_{pM}, it can be identified as the specific impedance of the medium $\rho c'$, where ρ is the density of the medium and c' is the speed of sound in the mesh. It must be considered that the speed of sound in the mesh is not necessarily the same as the theoretical speed of sound c. Assuming a homogenous discretization of the mesh ($\Delta x = \Delta y$), the speed of sound in the mesh can be calculated as $c' = \Delta x/\Delta t$. In accordance with the Courant condition and assuming this condition as equality, after some simple algebraic manipulations, the specific impedance of the DWM is

$$Z_{pM} = \rho c\sqrt{2}. \tag{18}$$

It has to be noted how this equivalence is true and constant in a dispersion-free frequency range. It has been assumed the performance of this algorithm is done up to a quarter of the sampling frequency, as stated in section 3.2, where the numerical speed of sound can be considered constant.

With the convenient arrangement of those cited elements, the whole mesh with a boundary condition is presented in Figure 4. The boundary condition is assembled to the DWM through a dummy junction. However, in this case, the DWM variables that connect this dummy junction to the impedance is converted to WDF variables through a simple scaling factor. These WDF ports are adapted in order to avoid reflections due to the port impedances mismatch. Once the WDF ports have adapted their impedance, they are conveniently filtered by a digital filter that represents the local impedance.

4.4. Analysis of the system

In this section, the system presented in section 4.3 is being analyzed in detail to demonstrate analytically that this model (Figure 4) works as a locally reacting impedance. This analysis is carried out in two directions: from the DWM variables to the digital filter and vice versa.

For purpose of analysis, let us consider the following example: a second order IIR digital filter modelling a discrete point of a plane surface with a normal vector in the x-direction and an impedance $Z(n)$. Let us define $a_M(n)$ and $b_M(n)$ as the outgoing and incoming WDF variables obtained from the dummy junction to wave variables, according equations (15) and (16). These variables have a specific impedance Z_{pM}. Then, they are adapted to the WDF specific impedance of the digital filter Z_{pI} [30], through the adapter (see equation 17). Then, a more suitable transformation of the adaptor equation should be made, where the WDF port variables in the impedance ($a_I(n)$ and $b_I(n)$) are obtained in terms of the WDF port variables in the mesh. With some simple algebraic manipulations, such wave variables become

$$a_I(n) = \alpha_M^- a_M(n) + \alpha_M^+ b_M(n), \tag{19}$$

$$b_I(n) = \alpha_M^+ a_M(n) + \alpha_M^- b_M(n), \tag{20}$$

where $\alpha_M^+ = (Z_{pM} + Z_{pI})/(2Z_{pM})$ and $\alpha_M^- = (Z_{pM} - Z_{pI})/(2Z_{pM})$

Substituting equations (15) and (16) into equations (19) and (20), WDF variable at the filter entrance can be obtained as a function of the DWM variable of the dummy

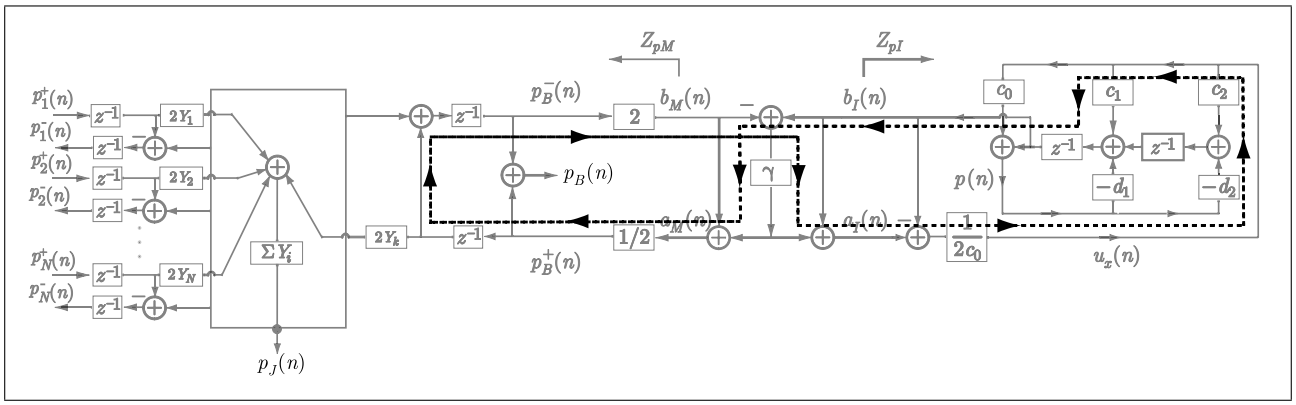

Figure 5. Scheme used for the analysis of the stability of a generic multidimensional W-DWM system, including update equations, interacting with the proposed model, where Y_k are the port admittances of the scattering junction J. The main loop able to produce a non computable system is indicated by a dashed line.

junction

$$a_I(n) = \left(p_B^+(n) + p_B^-(n)\right) + \frac{Z_{pI}}{Z_{pM}}\left(p_B^-(n) - p_B^+(n)\right), \quad (21)$$

$$b_I(n) = \left(p_B^+(n) + p_B^-(n)\right) - \frac{Z_{pI}}{Z_{pM}}\left(p_B^-(n) - p_B^+(n)\right). \quad (22)$$

Finally, from equations (21) and (22), and in accordance with Figure 4 and equation (9), the input of the filter is calculated as

$$\frac{a_I(n) - b_I(n)}{2Z_{pI}} = \frac{p_B^-(n) - p_B^+(n)}{Z_{pM}}. \quad (23)$$

In accordance with the equivalence of the plane waves in a DWM stated in section 3.2, and particularly, with equation (5), the entrance in the digital filter matches with the x-component of the particle velocity, which contains an inherent information regarding the angle of arrival θ

$$\frac{a_I(n) - b_I(n)}{2Z_{pI}} = \frac{\tilde{p}_{\text{inc}}(n) - \tilde{p}_{\text{ref}}(n)}{\rho c}\cos\theta. \quad (24)$$

It should be considered that equation (5) can be applied to the dummy junction without any change in its formulation, since only normal component to the wall can be applied to the dummy junction, being consistent with equation (23).

Now, the next step is to demonstrate that the output of the filter $p(n)$ is directly the pressure at the junction p_B. According to Figure 4 and WDF theory, and taking into account $Z_{pI} = c_0$ (see section 4.2)

$$a_I(n) = p(n) + Z_{pI}u_x(n), \quad (25)$$

$$b_I(n) = p(n) - Z_{pI}u_x(n). \quad (26)$$

The inverse of equations (19) and (20) can be useful for calculating the WDF ports in the mesh, $a_M(n)$ and $b_M(n)$):

$$a_M(n) = \alpha_I^- a_I(n) + \alpha_I^+ b_I(n), \quad (27)$$

$$b_M(n) = \alpha_I^+ a_I(n) + \alpha_I^- b_I(n), \quad (28)$$

where $\alpha_I^+ = (Z_{pI} + Z_{pM})/(2Z_{pI})$ and $\alpha_I^- = (Z_{pI} - Z_{pM})/(2Z_{pI})$.

Inserting equations (25) and (26) into equations (27) and (28), the following equations are obtained,

$$a_M(n) = p(n) + Z_{pM}u_x(n), \quad (29)$$

$$b_M(n) = p(n) - Z_{pM}u_x(n). \quad (30)$$

Once these equations are converted into DWM variables through the scaling factors, they become:

$$p^-(n) = \frac{p(n) + Z_{pM}u_x(n)}{2}, \quad (31)$$

$$p^+(n) = \frac{p(n) - Z_{pM}u_x(n)}{2}. \quad (32)$$

Then, these variables are related to the pressure $p_B(n)$ just adding both,

$$p_B(n) = p^+(n) + p^-(n) = p(n). \quad (33)$$

In order to check the stability of the system, it should be analyzed the possibility of appearing a delay-free loop: a purely digital network containing feedback loops are no longer computable because the computation of those loops in the discrete-time cannot be executed by a sequential procedure, due to the lack of pure delays along the loop. Figure 5 shows a graph which represent a loop which may produce instabilities due two interconnected explicit digital filters [11]. As it is observed from the figure, that loop contains a set of delays avoiding the unique source of instabilities in the interaction of both WDF systems.

It should be noticed how apparently the boundary condition implementation could seem more complex compared to the simplicity of the Huopaniemi's method. However, each part of the boundary condition structure must appear since the different nature of the variables (wave variables in the DWM and kirchhoff/physical variables of the digital filter) should be adapted through KW-pipes. Furthermore, in order to avoid instabilities, the impedance port adaptation must be included [36]. Therefore all parts are necessary in this structure. A way to reduce the computational cost could be by using efficient WDF impedance structures such as the ones recently proposed by Karjalainen [37].

5. Experiments and results

In order to demonstrate the validity of the proposed method in a cartesian mesh, some examples are presented. They correspond to the simulation of a frequency-dependent impedance surface, where the measured reflection factor is analyzed and compared with the theory at different angles. With the same set-up, some simulations are carried out with an interpolated cartesian mesh as well. Finally, some additional issues are addressed.

5.1. Experimental set-up

The experiment presents the effect of one impedance surface when plane waves strike it at different angles of incidence. Let us consider a 2-D mesh with 2000×1000 cells in a cartesian topology, where the boundary condition is implemented on the middle of the largest side and with a length of 1000 cells. The rest of the boundaries have been treated with absorbing boundary conditions [38] to reduce the presence of reflections coming from the limits of the mesh. The size of the cells is determined using the Courant formula as an equality. The sampling frequency is 80 kHz, and from now on the frequency axes are presented normalized to the sampling frequency. A Ricker wavelet with a normalized broadband of 0.25 has been selected as source [39]. These frequency limits have been selected in order to reduce, by over-sampling, the effects of the dispersion in the results, maintaining a compromise between accuracy and efficiency [2]. Although the theory assumes a plane wave source, a point source has been used for simplicity; this source has been situated far enough from the boundary in order to be considered as a plane wave when striking at the boundary [40]. In the results it will be shown how this point source consideration does not affect, even in low frequencies. Also, the $1/\sqrt{r}$ law has been compensated, where r is the distance between the source and the boundary.

In these simulations, the reflecting factors are obtained and they are analyzed and compared with theoretical results as a function of the angle of incidence. These measured reflection factors are obtained as a difference between the spectrum of an incident plane wave source and the measured reflected signal. A total-field/scattering-field formulation has been used in order to minimize undesirable reflection effects [41, 42]. This formulation consists of carrying out two simulations with the same initial conditions, but one with the proposed boundary condition and the other one without it. The scattering/reflecting field consists on the difference between both simulations. Besides, a proper analysis window size according to the length of each one of the reflected impulse responses have been chosen in order to avoid the presence of undesirable reflections.

For illustrative purposes, the frequency-dependent boundary condition is modelled as a hard-backed layer of porous material, described by Delany and Bazley's semi-empirical expressions [43]. In the following simulations a 0.1 m layer of porous material with a flow resistivity of 1000 kg/m^3/s is considered. The complex impedance components are represented in Figure 6. In accordance with the locally reacting impedance definition, equation (3), the theoretical reflection factor can be theoretically calculated for different angles. In this case, the angles of arrival under study θ are 0, 15, 30, 45, 60 and 75 degrees. These theoretical reflection factors are indicated in Figure 7.

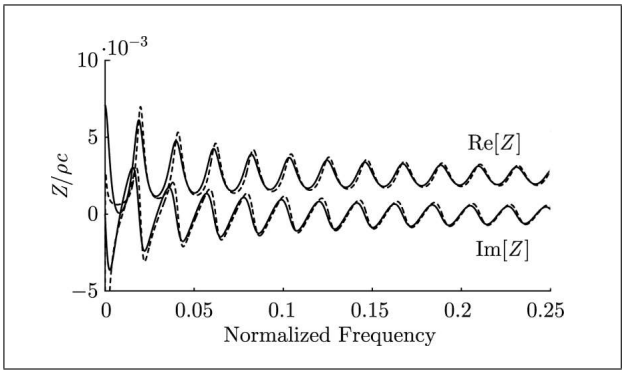

Figure 6. Complex impedance of a hard-backed layer of porous material, where the continuous line represents the theoretical impedance, whereas the dashed line is the complex spectrum of digital filter used to approach the impedance.

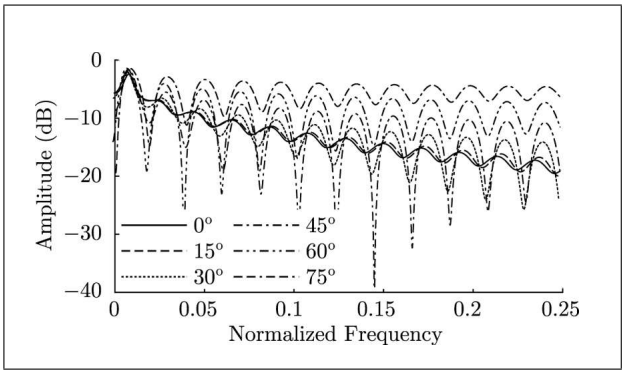

Figure 7. Theoretical reflection factor calculated for different angles of arrival, according to the analytical expression for a locally reacting impedance assumption.

The presented model is implemented and compared not only with the expected reflection factors obtained analytically, but also with the method that uses a digital filter representing the reflection factor (Huopaniemi's method in the sequel) [5].

The coefficients of the digital filter that represent the impedance have been modelled using an IIR digital filter of 60th order whose coefficients have been calculated according to Prony's algorithm using the analytical response of the absolute value impedance. Figure 6 also presents the complex components of the filter approach used to simulate the impedance. In the case of the Huopaniemi method, the reflection factor has been calculated from the locally reacting impedance definition and assuming a normal incidence ($\theta' = 0$). The corresponding digital filter coefficients have been calculated using a 60th order IIR filter

using Prony's algorithm as well, for representing the reflection factor at $\theta = 0$ (see Figure 7) [1].

5.2. Analysis of results

In accordance to the simulation configuration described above, a set of simulations have been performed. In Figure 8, the reflection factors at the specified angles are presented. The reflection factor obtained according the proposed method (solid line) is compared to the results obtained following the Huopaniemi method (dashed line) and with the expected theoretical results (dotted line). Although the Huopaniemi method has some dependence on the angle of arrival, it is too far from a locally reacting impedance [8]. However, the results obtained from the proposed method show an evident agreement with the expected results. It is true that some errors appear for high frequencies, but they are expected since for frequencies near to 0.25, dispersion effects are presented for most angles of propagation, except for $\theta = 45$ degrees (Figure 8d). For this particular scenario dispersion error is minimized, since at this angle the wave speed in the mesh matches that assumed in equation (18). At this angle, the inherent angular dispersion is minimized, independently of the oversampling used to reduce the frequency dispersion, and for that reason there is a high level of agreement between theory and results. For very low frequencies some discrepancies appear, but they are dependent on the window analysis size and the signal truncation.

This method only requires the definition of just one filter, the impedance filter, even when the reflection factor is largely dependent on the angle of arrival and the spectrums are highly different between them. This is one of the advantages with respect to the Huopaniemi method [5], because even with prior knowledge of the angle of arrival, it would be necessary to define a digital filter for each one of the possible angles. This would increase the computational cost and even in that case, the proper results would not be assured [8].

However, one of the main problems with this implementation is the efficiency of the W-DWM itself (see section 2). Fortunately, the global efficiency of the system can be augmented using a hybrid mesh in the fashion of [7] and [29]. As pointed out in section 2, generally, a hybrid mesh consists of a K-DWM realisation of the entire geometry and an interface with a W-DWM at the boundaries. The proposed method can be included in this hybrid mesh by simply coupling the model of Figure 4 with a K-DWM via the KW-pipe proposed in [15] (or with a more efficient version of this converter [6]) or the one in [29], more appropriated for the triangular DWM case.

At this point, some new simulations have been carried out under a hybrid mesh. However, since the KW-pipes have caused no errors [7, 29], the simulation carried out with this mesh have provided exactly the same result as using a W-DWM for the entire mesh. For that reason, no additional results are reported. Nevertheless, an interesting additional advantage of using KW-pipes is to couple an interpolated cartesian mesh (see Figure 9). The interpolated mesh itself does not reduce the frequency dispersion; however it spreads the angular dispersion evenly and then, combining it with warping filtering, the dispersion is reduced considerably [44]. The application of this mesh to room acoustic simulation has been frequently used [45, 46]. These results are presented in Figure 9 (solid line) and compared to the expected analytical result; and it can be observed how this mesh, with any additional consideration for the boundary condition, is directly coupled to the proposed boundary condition. However, not just one boundary junction has to be taken into account in this case, but also the boundary junctions situated in the diagonal in respect to the scattering junction p_J, with their respective weights, according to Reference [44]. The results show how for high frequencies some differences exist in respect to the theory, similar to the cartesian mesh; however the spectrum shape is still highly similar. These results demonstrate how the use of the proposed method is also suitable for alternative mesh geometries, such as the interpolated cartesian mesh.

5.3. Additional remarks

It should be mentioned that the idea of interfacing these paradigms had already been proposed by Karjalainen [12], where in order to achieve a 1-D simulation, an interface between FDTD (or K-DWM), DWG and WDF was proposed. However, this paper has demonstrated how this sort of interfacing provides additional advantages in a multidimensional simulation.

Another important feature to be considered is the linearity of the system. This is assured by the linearity of the digital filter and the interaction with the DWM. Let us assume two different plane waves with a different angle of arrival. If Huopaniemi's method is used with prior knowledge of the angle of arrival, it will be problematic because just one freedom degree exists in the digital filter design [8] and then, one of the plane waves would be filtered with an improper reflection factor filter. However, with the suggested method, this is not a problem because the impedance is constant with the angle of arrival and the system linearity permits the acquisition of a composition of reflected wave as if each one were obtained separately.

Observing the proposed boundary structure, it could be classified as a 1-D boundary condition [29], since only an adjacent scattering junction is involved for obtaining the pressure value at the boundary. However, although 2-D (or 3-D) boundary structures could be suggested for other implementations, this structure is consistent with the locally reacting impedance: it depends only on the *local* sound variables (obtained only from that adjacent scattering junction) and furthermore, the information required as input of the impedance digital filter is the normal component of the particle velocity, which is directly obtained in a 1-D structures, and not with 2-D structures since they in-

[1] Although it is true that 10 cm of porous absorbing material hardly reacts locally at frequencies of several kHz, Fig. 7 shows that the reflection factor has a considerable variability with the angle of arrival, which is higly illustrative for the purpose of this example.

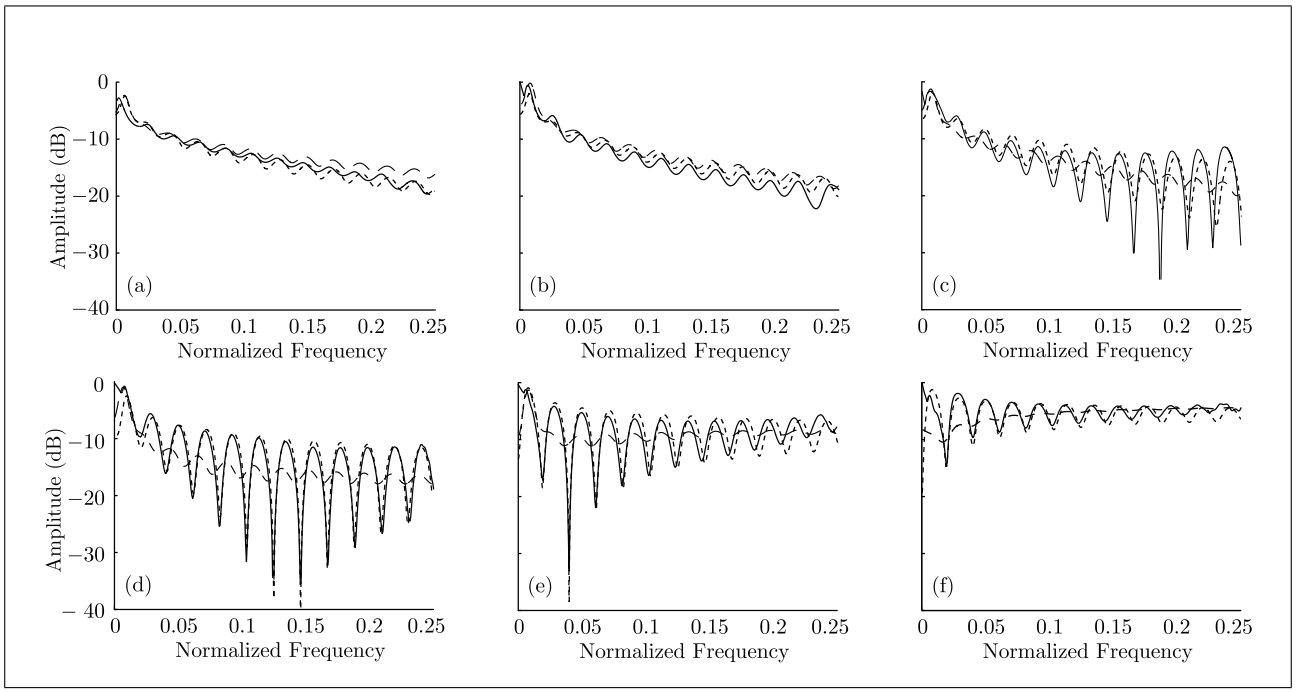

Figure 8. Reflection factors calculated with the proposed method for the cartesian mesh (solid line) and with the Huopaniemi's method [5] (dashed line), compared with the expected theoretical reflection factor (dotted line), for the angles: (a) 0 degrees, (b) 15 degrees, (c) 30 degrees, (d) 45 degrees, (e) 60 degrees, (f) 75 degrees.

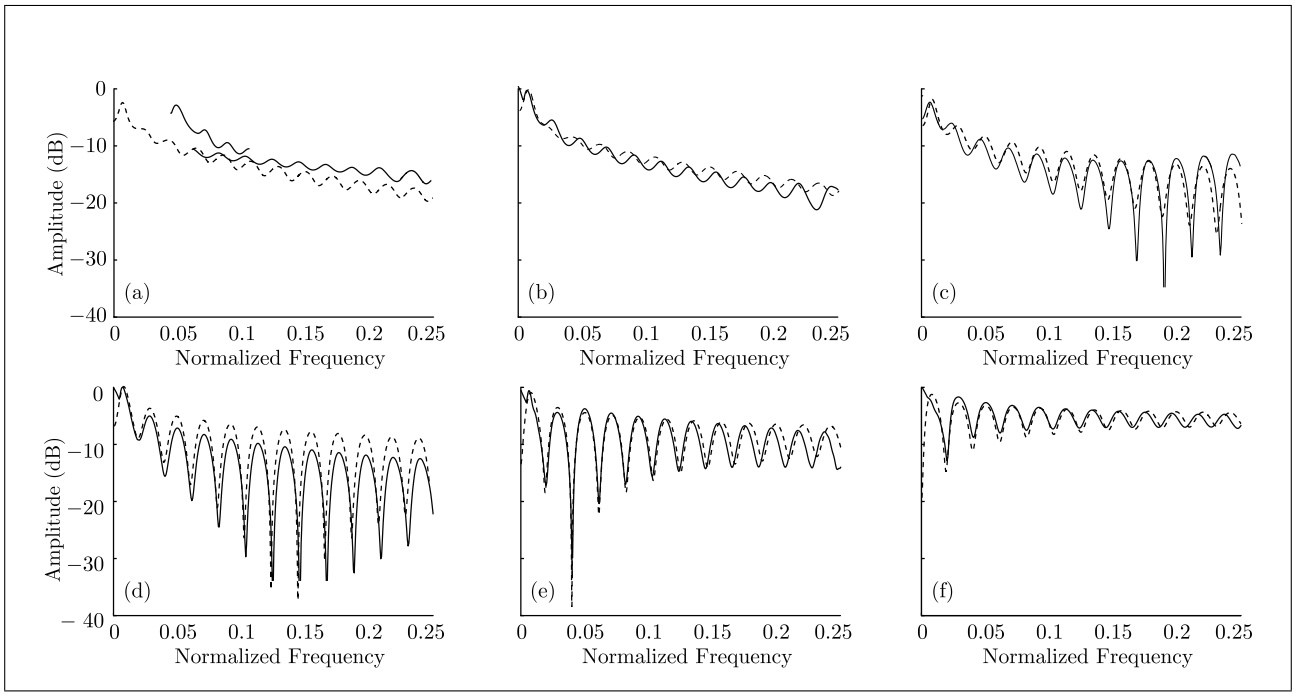

Figure 9. Reflection factors calculated with the proposed method for the interpolated cartesian mesh (solid line) compared with the expected theoretical reflection factor (dotted line), for the angles: (a) 0 degrees, (b) 15 degrees, (c) 30 degrees, (d) 45 degrees, (e) 60 degrees, (f) 75 degrees.

volve more scattering junction than the local one and the normal component does not requires more scattering junctions than the one situated at the normal direction.

It should be noticed that this model makes sense in a multidimensional simulation, where the concept of the angle of arrival appears. In case of 1-D simulations, the equation (3) has $\theta = 0$ and then, the same results are obtained with the previous approach as with the proposed model. However, in this particular case, the use of Huopaniemi's approach is more efficient than the presented one [7], since the coupling with the digital filter representing the reflection factor does not need any kind of adaptation.

One of the main limitations with this implementation may be the efficiency of the W-DWM itself. Fortunately, the global efficiency of the system can be augmented using a hybrid mesh in the fashion of [7] and [29]. Generally, a hybrid mesh consists on a K-DWM implementation of the entire geometry and an interface with a W-DWM at the boundaries. The proposed method can be included in this hybrid mesh by simply coupling the model of Fig. 4 with a K-DWM via the KW-pipe proposed in reference [15] (or with a more efficient version of this converter [6]) or the one in reference [29]. However, despite some similarities of this proposed method with reference [25], it should be considered how the former/new model does not require computation of the particle velocity components, whereas the latter does, increasing its memory storage.

Finally, it should be observed that the efficiency of that impedance model lies on the fact that the particle velocity components are not computed anymore. Therefore, if an impedance in the discrete-time (i.e. IIR structure) requires N components in the numerator and M components in the denominator ($M > N$), it is possible to implement digital filters with some efficient structures (i.e. direct form II, see reference [23]) requiring to store only M components per filter. Moreover, there exist some interesting alternatives for the implementation of WDF impedances able to reduce not the memory storage, but the computational cost [37].

6. Conclusion

In this paper, an efficient realisation for accurate specular reflections in a Digital Waveguide Mesh has been presented. Although mixed modelling is not a new idea in physical modelling of acoustic systems, the work presented has employed it to build a successful model for a locally reacting impedance in a multidimensional DWM. The use of a digital filter realisation of the impedance arises, instead of the reflection factor, as a proper solution to the problem, which agrees with the locally reacting impedance assumption. A digital filter structure of the impedance, based on the use of the Wave Digital Filters and a proper adaptation with the DWM method has been proposed. Different simulations have been carried out showing great accuracy with the theoretical model of a locally reacting impedance. In particular, it has been proven that the proposed method outperforms previously proposed methods, especially in the influence of the plane angle of arrival.

Acknowledgements

This work was supported by the Spanish Ministry of Science and Technology (MCYT) under Project reference TEC2006-13883-C04-01 and by FEDER funds.

References

[1] D. T. Murphy, A. Kelloniemi, J. Mullen, S. Shelley: Acoustic modeling using the digital waveguide mesh. IEEE Signal Processing Magazine **24** (2007) 55–66.

[2] S. A. Van Duyne, J. O. Smith: Physical modeling with the 2-d digital waveguide mesh. Proc. of the 1993 International Computer Music Conference (ICMC'93), Tokyo, Japan, 1993, 40–47.

[3] L. Savioja, J. Backman, A. Järvinen, T. Takala: Waveguide mesh method for low-frequency simulation of room acoustics. Proc. 15th Int. Congr. Acoust. (ICA'95), Trondheim, Norway, 1995, 637–640.

[4] D. Botteldooren: Finite-difference time-domain simulation of low-frequency room acoustic problems. J. Acoust. Soc. Am. **98** (1995) 3302–3308.

[5] J. Huopaniemi, L. Savioja, M. Karjalainen: Modelling of reflections and air absorption in acoustical spaces - a digital filter design approach. IEEE Workshop on Applications of Signal Processing to Audio and Acoustics (WASPAA'97), New York, USA, 1997.

[6] A. Kellomiemi: Frequency-dependent boundary condition for the 3-D digital waveguide mesh. Proc. of the 9th Int. Conference on Digital Audio Effects (DAFx-06), Montreal, Canada, 2006.

[7] M. Karjalainen, C. Erkut: Digital waveguides vs. finite difference schemes: equivalence and mixed modeling. Eurasip J. Applied Sig. Proc. **7** (2004) 978–989.

[8] J. Escolano, F. Jacobsen: A note on the physical interpretation of frequency dependent boundary conditions in a digital waveguide mesh. Acta Acustica united with Acustica **93** (2007) 398–402.

[9] S. Shelley, D. T. Murphy: The modeling of diffuse boundaries in the 2-D digital waveguide mesh. IEEE Trans. on Speech and Audio Processing **16** (2008) 651–665.

[10] A. D. Pierce: Acoustics: An introduction to its physical principles and applications. Acoustical Society of America,, Woodboury, NY, USA, 1991.

[11] A. Fettweis: Wave digital filters: theory and practice. Proceedings of the IEEE **74** (1986) 270–327.

[12] M. Karjalainen: Mixed physical modeling: DWG +FDTD +WDF. Proc. of the IEEE Int. Conf. on Acoustics, Speech, and Signal Processing (ICASSP'03), New Platz, NY, 2003.

[13] J. O. Smith III: Physical modelling using digital waveguides. Computational Music J. **16** (1992) 74–91.

[14] T. Laakso, V. Välimäki, M. Karjalainen, U. Laine: Splitting the unit delay-tools for fractional delay filter design. IEEE Signal Processing Magazine **13** (1996) 30–60.

[15] C. Erkut, M. Karjalainen: Finite difference method vs. digital waveguide method in string instrument modeling and synthesis. Proc. ISMA 2003, Mexico City, 2002.

[16] V. Välimäki, J. Pakarinen, C. Erkut, M. Karjalainen: Discrete time modeling of music instruments. Reports of Progress in Physics **69** (2006) 1–78.

[17] L. Savioja, T. J. Rinne, T. Takala: Simulation of room acoustics with a 3-D finite difference mesh. Proceedings of the International Computer Music Conference (ICMC'94), Aarhus, Denmark, 1994, 463–466.

[18] D. T. Murphy: Digital waveguide mesh topologies in room acoustics modelling. Ph.D. dissertation, University of York, UK, 2000.

[19] F. Fahy: Foundations of engineering acoustics. Academic Press, 2001.

[20] L. L. Beranek: Acoustic impedance of comercial materials and the perfomance of rectangular rooms with one treated surface. J. Acoust. Soc. Am. **12** (1940) 14–23.

[21] T. F. W. Embleton, J. E. Piercy, N. Olson: Outdoor sound propagation over ground of finite impedance. J. Acoust. Soc. Am. **59** (1976) 267–277.

[22] H. Kuttruff: Room acoustics. 4th ed. Spon Press, New York, 2000.

[23] J. G. Proakis, D. G. Manolakis: Digital signal processing. 3rd ed. Prentice-Hall, New Jersey, USA, 1996.

[24] F. Fontana, D. Rocchesso: Signal-theoretic characterization of waveguide mesh geometries for models of two-dimensional wave propagation in elastic media. IEEE Trans. on Speech and Audio Processing **9** (2001) 152–161.

[25] J. Escolano, F. Jacobsen, J. J. López: An efficient realisation of frequency dependent boundary conditions in an acoustic finite-difference time-domain model. J. Sound Vibr. **316** (2008) 234–247.

[26] G. de Sanctis, A. Sarti, S. Tubaro: Automatic synthesis strategies for object-based dynamical physical models in musical acoustics. Proc. of the 5th International Conference on Digital Audio Effects (DAFx-03), London, UK, 2003.

[27] M. Karjalainen, C. Erkut, L. Savioja: Compilation of unified physical models for efficient sound synthesis. Proc. of the IEEE Int. Conf. on Acoustics, Speech, and Signal Processing (ICASSP'03), New Platz, NY, 2003.

[28] R. Rabenstein, S. Petrausch, A. Sarti, G. De Sanctis, C. Erkut, M. Karjalainen: Block-based physical modeling for digital sound synthesis. Signal Processing Magazine **24** (2007) 42–54.

[29] D. T. Murphy, M. Beeson: The KW-boundary hybrid digital waveguide mesh for room acoustics applications. IEEE Trans. on Speech and Audio Processing **15** (2007) 552–564.

[30] S. Petrausch, R. Rabenstein: Interconnection of state space structures and wave digital filters. IEEE Trans. on Circuits and Systems II **52** (2004) 90–93.

[31] S. Petrausch, R. Rabenstein: Application of mixed modeling strategies for the simulation of the 2-D wave equation for arbitrary geometries. 15th European Signal Processing Conference, Poznan, Poland, 2007, 335–339.

[32] J. Szczupak, S. K. Mitra: Detection, localitation and removal of delay-free loops in digital filter structures. IEEE Trans. on Acoustics, Speech and Signal Proc. **23** (1975) 558–562.

[33] L. L. Beranek: Acoustics. McGraw-Hill, 1954.

[34] S. Petrausch, J. Escolano, R. Rabenstein: A general approach to block-based physical modeling with mixed modeling strategies for digital sound synthesis. Proc. of the IEEE Int. Conf. on Acoustics, Speech, and Signal Processing (ICASSP'05), Philadelphia, USA, 2005.

[35] M. Karjalainen: Discrete-time modeling and synthesis of musical instruments. Joint Baltic-Nordic Acoustics Meeting 2004, Mariehamn, Finland, 2004.

[36] S. D. Bilbao: Wave and scattering methods for the numerical integration of partial differential equations. John Wistley and Sons, 2004.

[37] M. Karjalainen: Efficient realization of wave digital components for physical modeling and sound synthesis. IEEE Trans. Audio, Speech and Language Processing **16** (2008) 947–956.

[38] D. T. Murphy, J. Mulle: Digital waveguide mesh modelling of room acoustics: improved anechoic boundaries. Proc. Sixth Conference on Digital Audio Effects (DAFx-02), Hamburg, Germany, 2002, 163–168.

[39] M. Vetterli, J. Kovacevic: Wavelets and subband coding. Ed. Prentice Hall Signal Processing Series, 1995.

[40] P. A. Butov: Reflection of a spherical wave from an impedance boundary. Sov. Phys. Acoust. **27** (1981) 191–193.

[41] K. R. Umashankar, A. Taflove: A novel method to analyze electromagnetic scattering of complex objects. IEEE Trans. Electromagnetic Compatibility **24** (1982) 397–405.

[42] G. Mur: Absorbing boundary conditions for the finite-difference approximation of the time-domain electromagnetic field equations. IEEE Trans. Electromagnetic Compatibility **23** (1981) 377–382.

[43] M. E. Delany, E. N. Bazley: Acoustical properties of fibrous absorbent materials. Applied Acoustics **3** (1970) 105–116.

[44] L. Savioja, V. Välimäki: Reducing the dispersion error in the digital waveguide mesh using interpolation and frequency-warping techniques. IEEE Trans. Speech and Audio Processing **8** (2000) 184–194.

[45] A. Kelloniemi, L. Savioja, V. Välimäki: Spatial filter based absorbing boundary for the 2-D digital waveguide mesh. IEEE Signal Processing Letters **12** (2005) 126–129.

[46] A. Kelloniemi: Improved adjustable boundary condition for the 2-D digital waveguide mesh. Proc. of the 5th Int. Conf. on Digital Audio Effects (DAFx'05), Madrid, Spain, 2005.